Ionic conductances contributing to spike repolarization and after-potentials in rat medial vestibular nucleus neurones

A. R. Johnston, N. K. MacLeod and M. B. Dutia*

Department of Physiology, Medical School, Teviot Place, Edinburgh EH8 9AG, UK

1. Intracellular recordings were made from 123 tonically active medial vestibular nucleus (MVN) neurones in a horizontal slice preparation of the dorsal brainstem of the rat. On the basis of their averaged action potential shapes, the cells were classified as either type A, having a single deep after-hyperpolarization (AHP; 40/123 cells, 33%), or type B, having an early fast AHP and a delayed slow AHP (83/123 cells, 67%). The two cell types were distributed throughout the rostrocaudal extent of the MVN.

2. In type A cells TEA reduced the single deep AHP and decreased the rate of spike repolarization. Depolarizing current pulses from a hyperpolarized membrane potential elicited spikes with short plateau potentials in TEA. These persisted in Ca^{2+}-free medium but were abolished along with the spontaneous activity in TTX. Ca^{2+}-free medium did not affect the initial rate of repolarization but reduced the deep AHP. Apamin and carbachol had little effect. 4-Aminopyridine (4-AP) slowed spike repolarization and the AHP amplitude by a small amount. Thus, in type A cells spike repolarization and AHP appear to be mediated largely by a TEA-sensitive potassium current (presumably I_K) and an apamin-insensitive Ca^{2+}-activated potassium current (presumably I_C).

3. The early fast AHP in type B cells was readily abolished in TEA. In seven of ten type B cells tested, the spontaneous spikes developed plateau potentials of 100–120 ms duration in 10 mM TEA, which then became 7–9 s long in Ca^{2+}-free medium. In the remaining three cells, the spontaneous plateaux were 1·75–2 s long in TEA, and were reduced to 30–100 ms in Ca^{2+}-free medium. TTX abolished the spontaneous spikes and plateaux. The delayed AHP was abolished by apamin, which induced irregular firing. 4-AP slowed spike repolarization and abolished the fast AHP, but did not induce plateaux. Thus, in type B cells spike repolarization involves a TEA-sensitive current (presumably I_K) as well as I_C and the 4-AP-sensitive potassium current I_A, while the apamin-sensitive potassium current I_{AHP} is responsible for the delayed AHP.

4. The tonic activity in type B cells appears to be regulated mainly by interactions between a persistent Na^+ current, which in most cells is large enough to generate plateaux when repolarization is impeded in TEA, and the hyperpolarization mediated by I_{AHP}. About 30% of type B cells have an additional inward Ca^{2+} current. In type A cells the persistent Na^+ current is either not large enough to generate plateaux or is more effectively counteracted by TEA-insensitive outward currents. The pacemaker conductances in type A and type B cells thus appear to be distinct.

Medial vestibular nucleus (MVN) neurones are the primary central targets of afferents from the ipsilateral horizontal semi-circular canal, and their projections to the oculomotor nuclei and the cervical spinal cord are amongst the most direct central pathways involved in the reflex control of the head and eyes (for reviews see Wilson & Melvil-Jones, 1979; Carpenter, 1988). The responsiveness of MVN cells to vestibular afferent inputs is modulated by reciprocal inhibitory interactions between the vestibular nuclei of the two sides, and by cerebellar Purkinje cell projections onto MVN neurones. Cervical proprioceptive and eye position signals also influence the activity of MVN neurones. These systems have been implicated in motor learning within the vestibulo-ocular reflex pathway, and may also be involved in bringing about the recovery of vestibular reflex function after peripheral vestibular

*To whom correspondence should be addressed.

lesions (Lisberger & Pavelko, 1988; Smith & Curthoys, 1989; Broussard & Lisberger, 1992).

The membrane properties of MVN neurones were first examined by Gallagher, Lewis & Shinnick-Gallagher (1985) in a transverse slice preparation of rat brainstem, and a number of subsequent studies have confirmed their finding that MVN neurones are intrinsically tonically active *in vitro* with spontaneous discharge rates similar to those observed *in vivo*. Most subsequent studies of the MVN *in vitro* have used extracellular recording techniques and have been concerned with determining the effects of various neurotransmitters and related substances on the tonic firing rates of MVN cells (e.g. Smith, Darlington & Hubbard, 1990; Dutia, Johnston & McQueen, 1992; Johnston, Murnion, McQueen & Dutia, 1993). Gallagher *et al.* (1985) (see also Gallagher, Phelan & Shinnick-Gallagher, 1992) pointed out that there were at least two subtypes of cell within the MVN, distinguishable on the basis of the after-hyperpolarizing potentials (AHPs) following their spontaneous action potentials. Serafin and co-workers (Serafin, de Waele, Khateb, Vidal & Muhlethaler, 1991*a*, *b*) subsequently formalized this by classifying guinea-pig MVN neurones into three types (A, B and C) based on their action potential shapes and intrinsic membrane properties *in vitro*. Type A cells (about 30%) were characterized by a broad action potential and a single deep AHP, while type B cells (about 50%) had narrower action potentials and showed an early fast AHP and a delayed slow AHP. Type C cells (about 20%) were heterogenous with intermediate action potential shapes and could not be readily included in the other two classes.

In the present study we have systematically examined the membrane properties and action potential shapes of 123 tonically active MVN neurones in a horizontal slice preparation of the dorsal brainstem of the rat. With the use of spike-shape averaging to reveal the AHPs present in each cell more clearly, all of the MVN cells recorded in this study were classified into two groups analogous with, but not identical to, the type A and type B groups of Serafin *et al.* (1991*a*). In addition the ionic conductances involved in spike repolarization and the AHPs in the two subtypes of MVN cell were characterized. The results indicate that different ionic mechanisms underlie the tonic activity and rhythmicity of the two subtypes of MVN cell, and suggest the possibility that type A and type B cells may be differentially sensitive to control by neuromodulatory systems within the brainstem.

METHODS

Slice preparation and recording

Slices of the dorsal brainstem were prepared from young male Sprague–Dawley rats weighing 100–225 g. The animals were anaesthetized in halothane (3% in oxygen) and decapitated by guillotine. The brain was removed into ice-cold artificial cerebrospinal fluid (ACSF; composition (mM): NaCl, 124; KCl, 5; KH_2PO_4, 1·2; $MgSO_4$, 1·3; $CaCl_2$, 2·4; $NaHCO_3$, 26·0; and D-glucose, 10·0). A block of tissue extending from the inferior colliculi to the obex was isolated, and the cerebellum removed so as to expose the floor of the fourth ventricle. The block was cemented to the stage of a Vibraslice (Camden Instruments, London), with the fourth ventricle uppermost and the obex facing the cutting blade. Slices of 400–450 μm thickness were cut in the horizontal plane, approximately parallel to the floor of the fourth ventricle (Dutia *et al.* 1992). The slices were transferred to an interface-type incubation chamber which was continuously perfused with ACSF equilibrated with 95% O_2–5% CO_2 (pH 7·4; flow rate, 1·6 ml min^{-1}) and maintained at 33·0 ± 0·2 °C. All slices were incubated for a minimum of 1 h before recording.

Intracellular recordings were made from medial vestibular nucleus neurones using conventional glass microelectrodes filled with 3 M potassium chloride (resistance 70–90 MΩ), connected to the head stage of an AxoClamp 2A amplifier (Axon Instruments, Foster City, CA, USA). A piezoelectric stepping motor (Inchworm model 6000; Burleigh Instruments Ltd., Harpenden, Herts, UK) was used to advance the microelectrode through the slice in 2 μm steps. Intracellular potentials were recorded using either the active bridge mode or discontinuous current-clamp mode of the AxoClamp amplifier, amplified and displayed conventionally, recorded on tape, and digitized on-line using a CED 1401 plus laboratory interface (Cambridge Electronic Design, Cambridge, UK) connected to an IBM-compatible computer. The interface was also used to generate current stimulus pulse protocols.

Drugs were made up to a known final concentration in ACSF and applied to the slice by switching the perfusion inlet tube to different reservoirs by means of three-way taps. Tetraethylammonium (TEA) chloride, 4-aminopyridine (4-AP), tetrodotoxin (TTX) and apamin were obtained from Research Biochemicals Inc. (Semat; St Albans, Herts, UK). In a number of experiments the normal Ca^{2+} concentration in the ACSF was lowered to 0·5 mM and supplemented with 0·5 mM $CoCl_2$ ('low-Ca^{2+} Co^{2+} medium', Jahnsen, 1980), or calcium was omitted entirely and replaced with 1 mM $CdCl_2$ ('Ca^{2+}-free Cd^{2+} medium', Llinás & Sugimori, 1980). In the latter case the NaH_2PO_4 and $MgSO_4$ were also omitted to avoid precipitation (Llinás & Sugimori, 1980).

Analysis of action potential shape in tonically active MVN cells

In order to examine the action potentials and after-potentials in MVN cells in detail, the intracellularly recorded membrane potential was digitized at 40 kHz for a period of 2 s while the cell fired spontaneous action potentials. Subsequently the time of occurrence of the peak of each action potential was located in the digitized data, and the membrane potential over a 20 ms window around each of these times was averaged to give an action potential shape synchronized to the peak of the spike (Fig. 1, upper trace). Averaged action potential shapes were obtained for MVN cells at their 'resting' membrane potentials (i.e. without any current injection through the recording microelectrode), and for a number of cells at different frequencies of discharge elicited by constant injection of hyperpolarizing or depolarizing current (for example see Fig. 3). Where quantitative values of 'resting membrane potential' are given below, these refer to the values of mean membrane potential (V_m) obtained from the front panel display of the AxoClamp amplifier.

Since the membrane potential in tonically active MVN cells was always gradually depolarizing before the discharge of an action potential, it was not possible to make an objective measurement of the firing threshold (the point of onset of the rising phase of the action potential) from the averaged spike shape itself. Instead the averaged spike shape was differentiated twice (Fig. 1, middle and lower traces), and the firing threshold was taken to be the membrane potential at the point when the second derivative became greater than 2 times its own noise level (Fig. 1, dashed lines). The action potential rise time was measured as the time from the firing threshold to the peak of the averaged action potential, and the fall time as the time to return from the peak to the threshold level (Fig. 1, upper trace). The amplitudes of after-hyperpolarizations were also measured with respect to firing threshold. The spike width was measured both as the width at threshold (W_T) and as the width at half-height (W_H, Fig. 1).

All values are given as means ± S.D. unless otherwise stated.

RESULTS

Intracellular recordings were made from 123 MVN neurones in eighty-one slice preparations. All the cells included here had resting membrane potentials greater than −50 mV, and fired spontaneous action potentials greater than 60 mV in amplitude ($A_{SP} + A_{AHP}$ (amplitude of AHP with reference to firing threshold plus spike amplitude) Fig. 1; 71·6 ± 7·9 mV), at steady rates between 3 and 60 impulses s^{-1} (27·1 ± 13·0 impulses s^{-1}). A further seven non-tonically active cells were also encountered, which had stable resting potentials of −60 to −65 mV and which could be made to fire tonically by depolarizing current injection; these silent cells are not included in the present data. As shown for example in Figs 5 and 9, in tonically active cells the spontaneous action potentials arose from a gradual membrane depolarization rather than synaptic potentials. Spontaneous postsynaptic potentials were observed in some MVN cells, where they interacted with the intrinsic membrane depolarization and occasionally interjected extra spikes into an otherwise steady discharge.

Cell types in the rat MVN

The spontaneous action potentials in tonically active MVN neurones occurring over a 2 s period were averaged in order to examine the action potential shape in detail (see Methods and Fig. 1). As shown in the examples in Figs 2 and 3, on the basis of their averaged action potential shapes MVN cells fell into two distinct groups. MVN cells in the first group showed a characteristic single deep AHP of 15–27 mV amplitude (20·43 ± 3·0 mV, $n = 40$; e.g. Figs 2*A* and 3*A*; see also Figs 5–7). During normal spontaneous activity in many of these cells the decay of the AHP was not continuous with the depolarization that led to the following spike (Fig. 3*A*, arrow; see also Figs 6 and 7). This discontinuity was less obvious when these cells were hyperpolarized close to their firing thresholds by current injection, and more so when depolarized so that they fired more frequently (Fig. 3*A*). Varying the cell membrane potential in this way had little effect on the amplitude of the characteristic deep AHP, but altered the rate of membrane depolarization leading to the succeeding spike.

The second group of MVN cells showed an early fast AHP and a delayed slow AHP which, although they were present in all cells in this group, varied in their relative

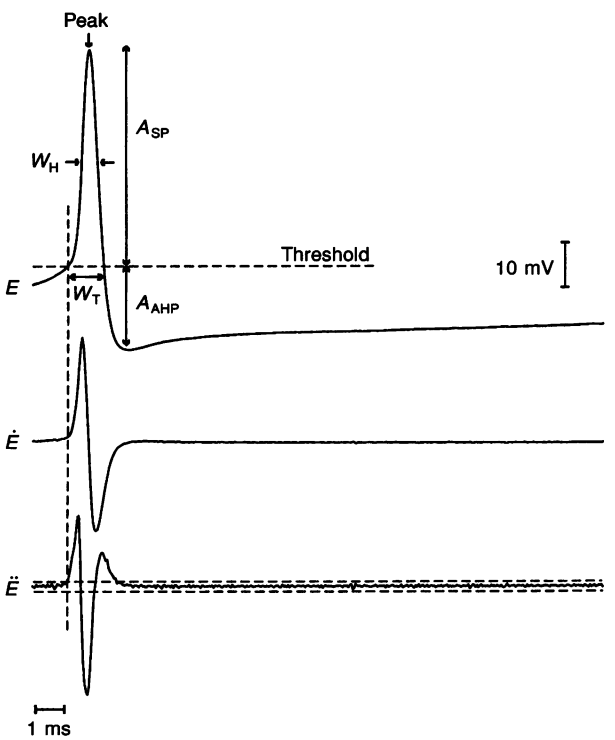

Figure 1. Analysis of averaged action potential shape
Upper trace, averaged action potential shape (E) obtained by averaging the membrane potential over a 20 ms window synchronized to the peak of each successive spike in the resting discharge of one MVN cell, with a 1·25 ms pre-trigger period (see text). Middle and lower traces, first ($\dot{E}$) and second ($\ddot{E}$) differentials of the averaged spike shape, calculated by taking simple differences between successive points. Horizontal dashed lines in the lower panel indicate the level corresponding to twice the noise amplitude in the last 5 ms of this trace. The vertical dashed line indicates where the second differential becomes greater than this level, and the corresponding point in the averaged spike shape (upper trace) which is taken as the onset of the rising phase of the action potential (firing threshold). W_T, spike width at firing threshold; W_H, spike width midway between firing threshold and peak; A_{AHP}, amplitude of AHP with reference to firing threshold; A_{SP}, spike amplitude. Rise time was measured as the time from firing threshold to peak, and fall time as the time from peak to firing threshold.

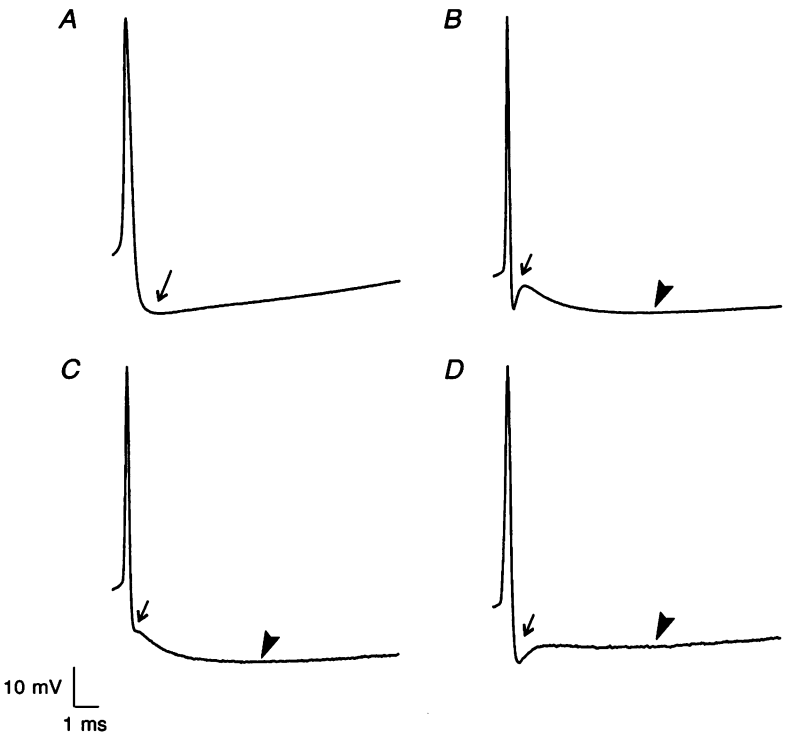

Figure 2. Spike-shape averaging reveals two subtypes of MVN cell
A–D, averaged action potential shapes of four different MVN cells. In this and subsequent figures, the averages are the result of 12–38 sweeps, unless otherwise indicated. Arrow in *A* indicates the single deep AHP characteristic of type A cells, and arrows in *B*, *C* and *D* indicate the early fast AHP (arrows) and delayed slow AHP (arrowheads) characteristic of type B cells.

prominence in different cells (Figs 2*B*, *C* and *D*; see also Fig. 3*B* and Figs 9–12). Although in many of these cells the two AHPs were directly apparent in the resting discharge without spike-shape averaging (e.g. Fig. 2*B*), in a substantial number of cells either the early fast AHP or the delayed slow AHP was not prominent enough to be observed directly and the presence of two AHPs was only clearly revealed through the averaging of successive action

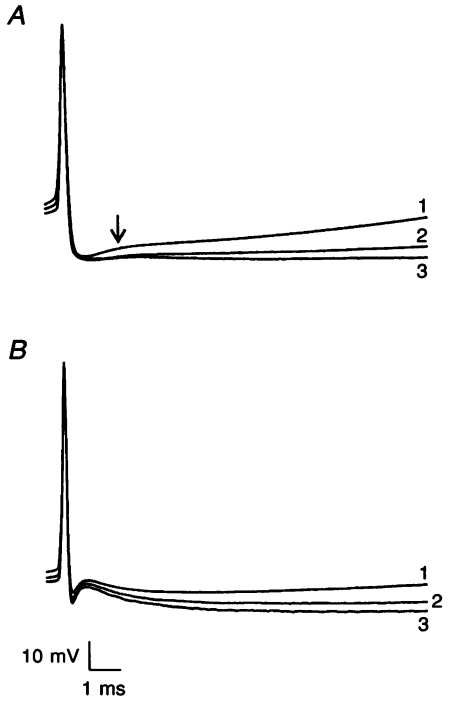

Figure 3. Effects of membrane potential on the spike shape of type A and type B MVN cells
Averaged action potential shapes from a type A cell (*A*), and a type B cell (*B*), at different levels of membrane potential. In *A*, trace 2 was obtained at the resting membrane potential and traces 1 and 3 were obtained during injection of depolarizing and hyperpolarizing current (+0·2 and −0·15 nA), respectively. In *B*, trace 1 was obtained at the resting membrane potential and traces 2 and 3 during hyperpolarizing current injection. The resting membrane potential of the cell in *A* was −56 mV and in *B* was −53 mV.

potentials (for example see Fig. 2*C* and *D*). As shown in Fig. 3*B*, slowing down the spontaneous discharge by hyperpolarizing current injection did not affect the early fast AHP, but increased the amplitude and duration of the delayed slow AHP (e.g. Fig. 3*B*, traces 2 and 3). Thus in cells with a clear fast AHP but where the delayed AHP was too small to be observed directly, hyperpolarization often increased the amplitude of this AHP sufficiently for it to be recognized without spike-shape averaging. However, for cells where the fast AHP was not directly apparent (e.g. Fig. 2*C*) spike-shape averaging was necessary to reveal the presence of two AHPs. There was no indication of an active after-depolarization following the first AHP in these cells either when the action potential shapes were examined at different levels of membrane potential (e.g. Fig. 3), or when the delayed slow AHP was selectively blocked by apamin (see below and Fig. 11).

These two groups of MVN cells correspond to the two main cell types observed by Gallagher *et al.* (1985), and to the type A and type B cells, respectively, in the classification proposed by Serafin *et al.* (1991*a*). Although Gallagher *et al.* (1985) reported intermediate action potential shapes in a minority of cells, and the classification of Serafin *et al.* (1991*a*) also included a third class of cells (type C) with intermediate properties, in the present study with the use of spike-shape averaging all the MVN neurones were clearly shown to have either a single AHP (type A cells) or an early fast AHP and a late slow AHP (type B cells). All of the silent (non-tonically active) cells encountered in this study were type B cells, as evidenced by their action potential shapes when they were depolarized to firing threshold by current injection. Of the 123 tonically active cells included here, 40 (33%) were classified as type A cells, and the remaining 83 (67%) as type B cells.

Characteristics of type A and type B MVN cells

Following the observation of Serafin *et al.* (1991*a*) that in a selected sample of guinea-pig MVN cells type A cells had significantly wider action potentials than type B cells, the action potential durations of all cells in the present study were systematically measured as the width at threshold (W_T), and as the width at half-height (W_H, see Methods and Table 1). Both measurements of action potential duration were found to overlap extensively, as shown for W_T in Fig. 4*A*. Nonetheless the mean spike width at threshold in type B cells was significantly shorter than in type A cells (Table 1). The spike widths at half-height were also similarly significantly different. The narrower action potentials in type B cells were due to their mean rise times and fall times being significantly shorter than in type A cells (Fig. 4*B* and *C*; Table 1). The membrane resistances of type A and type B cells (overall mean $61{\cdot}5 \pm 31{\cdot}7$ mΩ) and their membrane time constants (overall mean $11{\cdot}65 \pm 5{\cdot}32$ ms) did not show significant differences. Both type A and type B cells were found distributed through the rostrocaudal extent of the MVN, and there was no suggestion of a spatial segregation of the two cell types within the nucleus. The resting rates of discharge of all the cells included in this study are shown in Fig. 4*D*.

Ionic basis of spike repolarization and after-hyperpolarizations

Type A cells

The effects of selective potassium ion-channel blocking agents and calcium-substituted ACSF on the action potentials of sixteen type A cells were examined. One such experiment is illustrated in Fig. 5. The characteristic single deep AHP of the type A cell was markedly reduced in 10 mM TEA (Fig. 5*B* and *D*), and the rate of spike repolarization (measured as the average rate of change of voltage from peak to firing threshold, Fig. 1), was reduced from 149 to 37 V s^{-1} (Fig. 5*D*). This occurred uniformly over the falling phase of the action potential so that the action potential width increased both when measured at half-height (from 0·45 to 0·975 ms, W_H) or at firing threshold (from 0·95 to 2·435 ms, W_T). At its resting potential, the cell continued to fire broad action potentials at a steady rate (Fig. 5*B*, uppermost trace), but in response to small depolarizing current pulses from a hyperpolarized membrane potential the widening of the action potential was more pronounced and a secondary, smaller spike was often elicited before repolarization was complete (Fig. 5*B*, arrow). Unlike type B cells, however (see below), none of the type A cells generated long plateau potentials in TEA. The consequences of a slower repolarization and a wider action potential were seen in greater spike amplitude accommodation when the cell fired at higher rates of discharge in response to larger depolarizing current pulses

Table 1. Action potential width at firing threshold (W_T), action potential width at half-height (W_H), spike rise time and fall time for the two subtypes of MVN cell identified in this study

	W_T (ms)	W_H (ms)	Rise time (ms)	Fall time (ms)	*n*
Type A cells	$0{\cdot}84 \pm 0{\cdot}17$	$0{\cdot}42 \pm 0{\cdot}09$	$0{\cdot}46 \pm 0{\cdot}11$	$0{\cdot}38 \pm 0{\cdot}09$	40 (33%)
Type B cells	$0{\cdot}63 \pm 0{\cdot}17$	$0{\cdot}30 \pm 0{\cdot}07$	$0{\cdot}35 \pm 0{\cdot}09$	$0{\cdot}28 \pm 0{\cdot}10$	83 (67%)
P value	$<0{\cdot}001$	$<0{\cdot}001$	$<0{\cdot}001$	$<0{\cdot}001$	

The *P* values shown were obtained using a two-tailed Student's *t* test assuming unequal variances.

(Fig. 5*B*). In four cells where different concentrations of TEA were compared, 5 mM TEA was found to have only a slightly smaller effect on the rate of repolarization and AHP amplitude than 10 mM TEA, suggesting that the effects of 10 mM TEA are likely to be nearly maximal.

The rate of repolarization became still more prolonged and near-exponential in shape in Ca^{2+}-free Cd^{2+} medium containing 10 mM TEA (Fig. 5*C*, uppermost trace and Fig. 5*D*), and the action potential width increased further to 1·75 (W_H) and 4·65 ms (W_T). The secondary spikes elicited by depolarizing current pulses at a hyperpolarized potential were not abolished in Ca^{2+}-free Cd^{2+} medium, and instead the action potential developed a short plateau lasting 20–25 ms upon which a secondary spike occurred (Fig. 5*C*, arrows). The spiking activity during larger depolarizations showed more marked amplitude accommodation, so that large depolarizing pulses now completely inactivated the action potential (Fig. 5*C*). The action potentials, secondary spikes and plateau potentials were abolished in TTX (0·5 μM; not shown). Similar cumulative effects of TEA and Ca^{2+}-free Cd^{2+} medium on the rate of repolarization and the AHP amplitude were observed in six type A cells.

As shown for a second type A cell in Fig. 6, the characteristic single AHP was also reduced markedly in Ca^{2+}-free Cd^{2+} medium, and the rate of repolarization decreased from 120 to 51 V s^{-1}. In contrast to the effects of TEA, however, the initial rate of spike repolarization was relatively unaffected in Ca^{2+}-free medium so that W_H increased only from 0·525 to 0·6 ms, while the repolarization in the latter part of the spike was more affected and W_T increased from 0·925 to 1·275 ms (Fig. 6*C*). All of the type A cells exposed to Ca^{2+}-free medium either with or without TEA continued to fire tonically, and unlike type B cells (see below) did not show any tendency towards burst-like activity.

In three type A cells tested, the small conductance (SK)-type calcium-activated potassium channel blocker apamin (0·1–0·3 μM; Blatz & Magleby, 1986) had no detectable effect on the rate of spike repolarization and decreased the amplitude of the deep AHP by only a small amount (Fig. 7*C*). Nonetheless this was accompanied by an

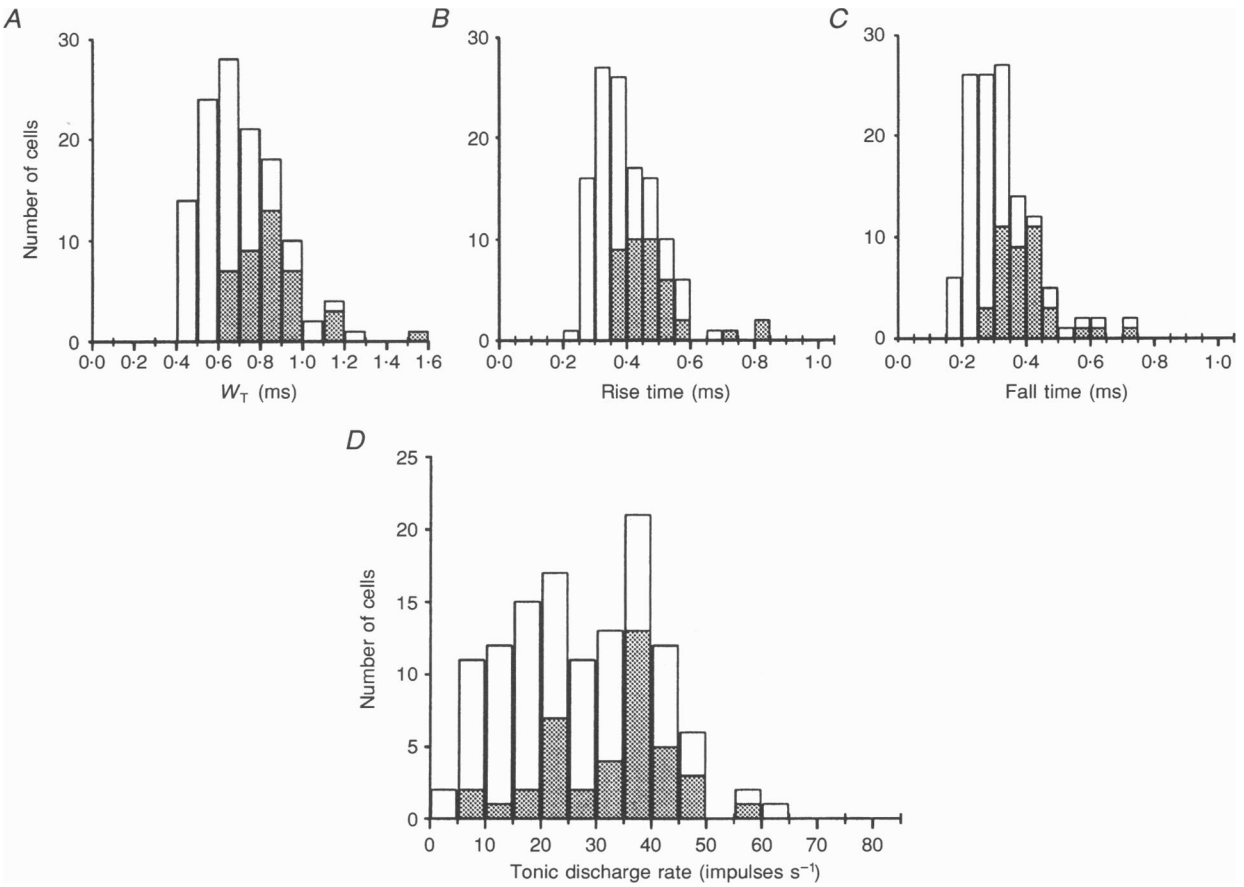

Figure 4. Action potential characteristics and firing rates of type A and type B MVN cells
Histograms showing the distribution of action potential width at firing threshold (W_T, *A*), rise times (*B*) and fall times (*C*) of type A (▨) and type B (□) cells. The resting firing rates of the two types of cells are shown in *D*.

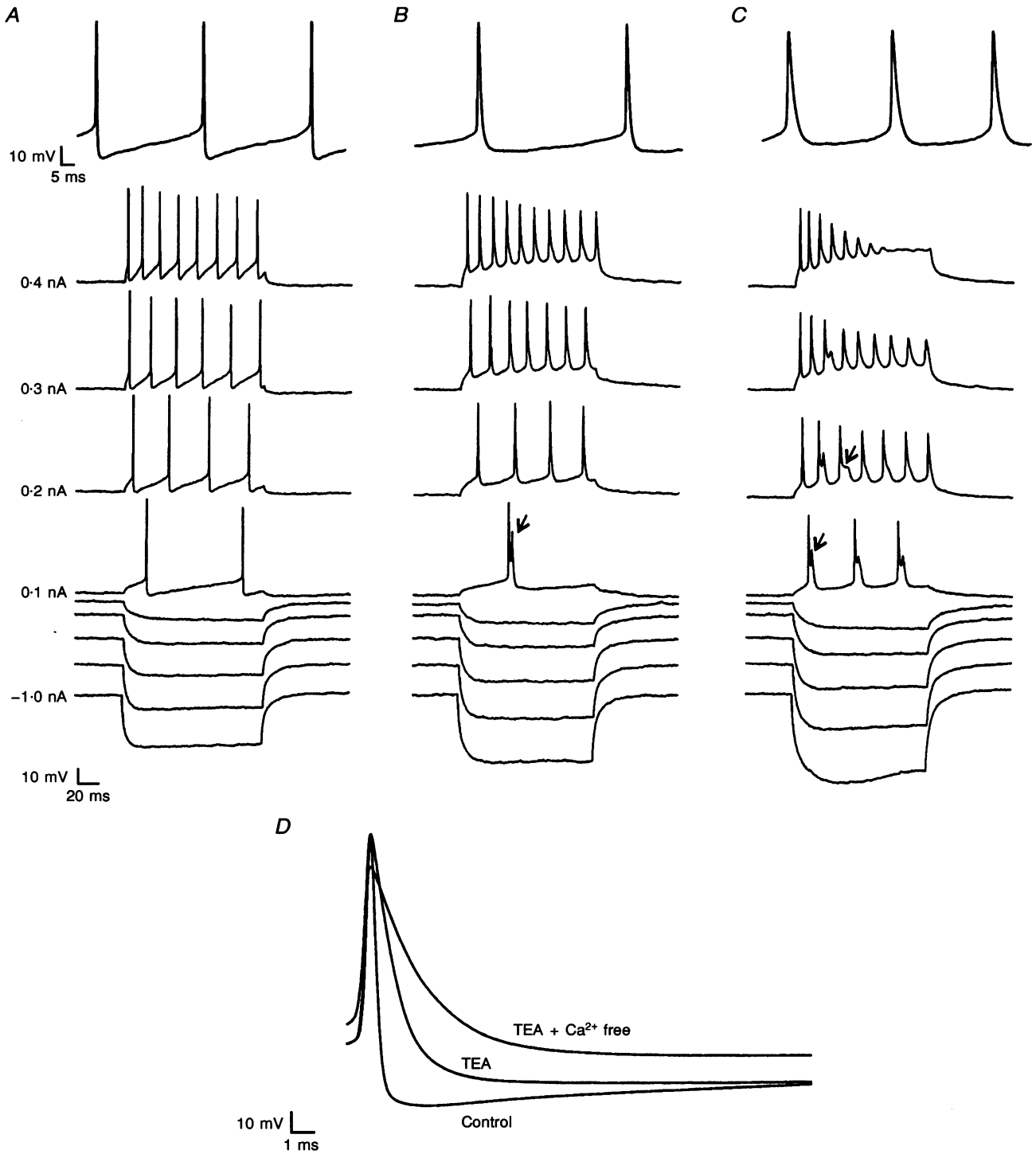

Figure 5. Effects of TEA and Ca^{2+}-free medium on action potential repolarization in a type A cell

A, resting discharge (uppermost trace) and responses to current pulses in normal ACSF. *B*, after 10 min in 10 mM TEA; and *C*, after 22 min in Ca^{2+}-free Cd^{2+} medium containing 10 mM TEA. The lower traces in *A*, *B* and *C* show responses to hyperpolarizing and depolarizing current pulses at a membrane potential of −65 mV. *D*, averaged spike shapes obtained during tonic activity in normal ACSF, 10 mM TEA and Ca^{2+}-free medium superimposed. Arrows in *B* and *C* indicate plateau potentials, some with secondary spikes, in TEA and Ca^{2+}-free medium, respectively.

appreciable decrease in membrane conductance, as evidenced by the larger voltage changes elicited in response to current steps (Fig. 7*B*). In three further type A cells tested with 4-AP at a concentration known to be sufficient to block A-type potassium currents in hippocampal pyramidal cells (0·5 mM; for example see Gustafsson, Galvan, Grafe & Wigstrom, 1982; Storm, 1987, 1990), the rate of repolarization was slowed by a small amount and the amplitude of the deep AHP reduced slightly (Fig. 8). However, 4-AP at this concentration did not affect the regularity of the tonic discharge and also did not affect the delay to the first action potential during a

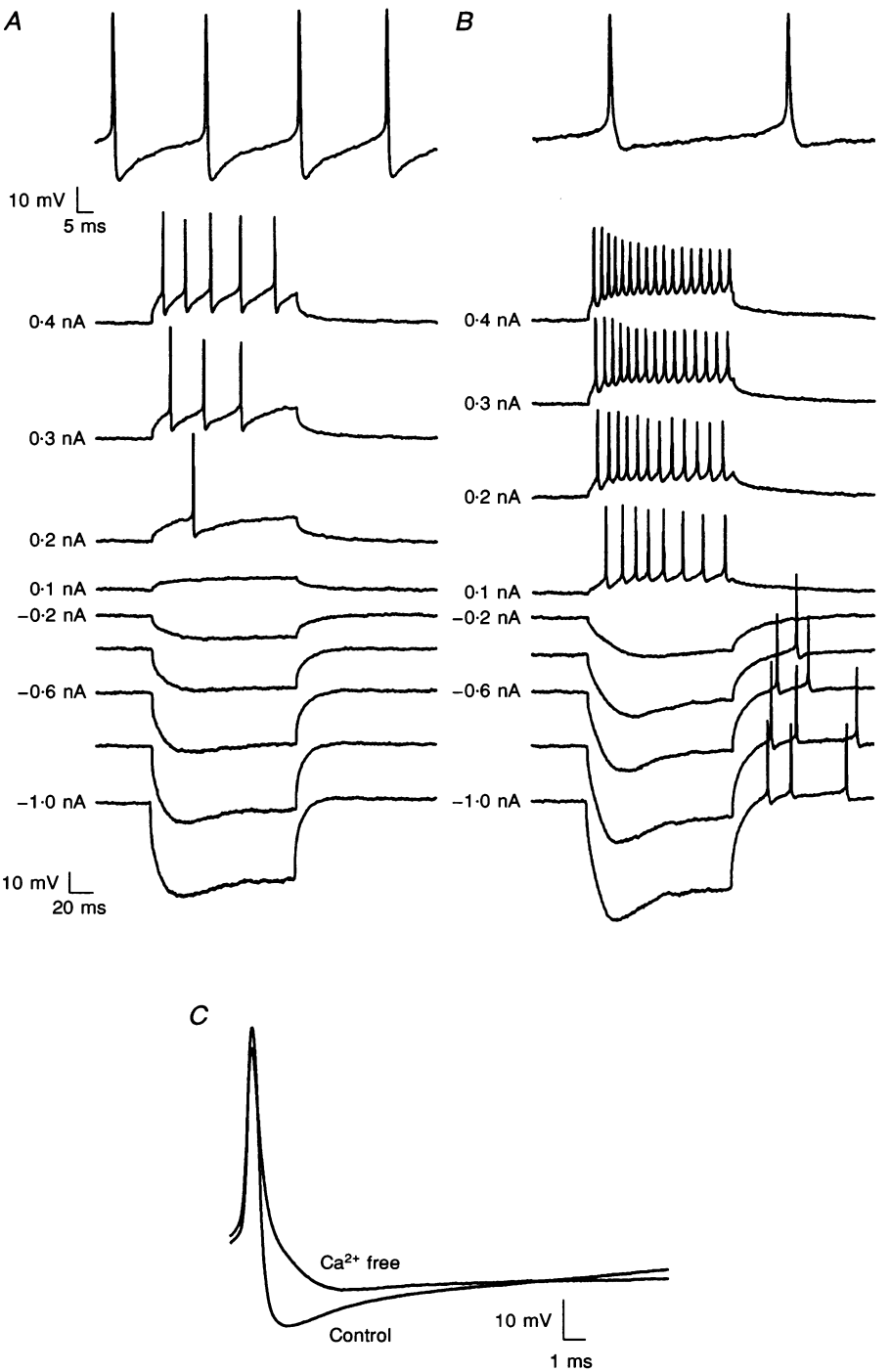

Figure 6. Effects of Ca^{2+}-free Cd^{2+} medium on action potential repolarization in a type A cell
A, resting discharge (uppermost trace) and responses to current pulses in normal ACSF; and *B*, after 20 min in Ca^{2+}-free Cd^{2+} medium. The lower traces in *A* and *B* show responses to hyperpolarizing and depolarizing current pulses at a membrane potential of −65 mV. *C*, averaged spike shapes obtained during tonic activity in normal ACSF and Ca^{2+}-free medium superimposed.

small depolarizing pulse from a hyperpolarized membrane potential. Higher concentrations of 4-AP gave rise to spontaneous membrane potential fluctuations, but did not have any greater effects on the rate of spike repolarization. Carbachol (50–100 μM), which is known to block the M-type potassium current (I_M) in hippocampal neurones (Halliwell & Adams, 1982), had no effect on the rate of repolarization or the amplitude of the deep AHP ($n = 2$).

Type B cells

Similar experiments using K^+ channel blockers and calcium-substituted media were carried out in thirty-one type B MVN cells. The effects of TEA on the tonic activity and action potential shape of a representative type B cell are shown in Fig. 9. The early fast AHP was readily abolished in 5 mM TEA, while the late AHP was not affected (Fig. 9*B* and *G*, traces 1 and 2). The rate of repolarization was slowed uniformly over the falling phase of the spike, from 220 to 63 V s^{-1}, and the spike width increased from 0·65 to 1·575 ms (W_T). In 10 mM TEA the rate of repolarization was slowed further, and within a few minutes W_T increased to 3–4 ms and a smaller secondary spike was elicited on top of a marked shoulder (Fig. 9*G*, trace 2). With continued equilbration in 10 mM TEA the shoulder became more pronounced until after about 10 min each action potential was followed by a plateau potential lasting about 30 ms (Fig. 9*G*, trace 4 and Fig. 9*C*, first two spikes). The cell continued to fire broad action potentials regularly at its resting membrane potential, but occasionally one of these spontaneous action potentials was followed by a plateau of over 1 s duration (Fig. 9*C*, third spike). At the end of a prolonged plateau of this sort the slow AHP was very much enhanced and persisted for 500 ms or more, interrupting the steady discharge. Injection of small depolarizing pulses from near the resting membrane potential always elicited an action potential with a prolonged plateau that lasted for 1 s or more

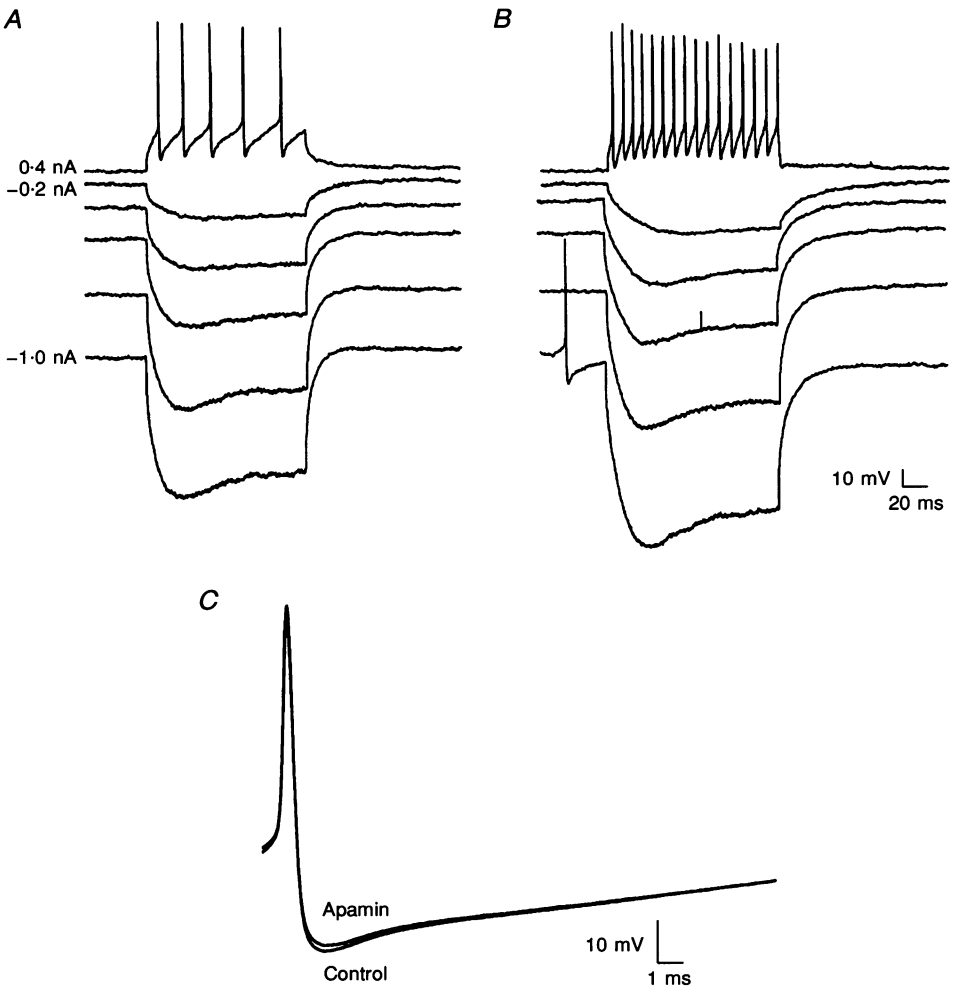

Figure 7. Effects of apamin on a type A cell
A, responses to current pulses at a membrane potential of −65 mV in normal ACSF; and *B*, after 12 min in apamin (100 nM). *C*, averaged spike shapes obtained during tonic activity in normal ACSF and in apamin superimposed. Note decrease in cell conductance evidenced by the larger voltage changes evoked by the current pulses in *B*, with only a small change in spike shape (*C*).

(Fig. 9*D*). Further current pulses applied during the plateau potentials elicited voltage changes of only a few millivolts in the cell membrane, indicating a sustained high-conductance state during the plateau.

In Ca^{2+}-free Cd^{2+} medium the plateau potentials were not abolished but instead became very much prolonged, the plateau during each of the spontaneous action potentials lasting 7–9 s (Fig. 9*E*). The deep long AHPs that followed the prolonged action potentials in normal medium plus TEA (Fig. 9*C*) were abolished in Ca^{2+}-free Cd^{2+} medium, so that the membrane potential began to depolarize again immediately after the repolarization at the end of the plateau (Fig. 9*E*, arrow). The spontaneous depolarizations, the action potentials and the plateau potentials were abolished when 0·5 μM TTX was added to the Ca^{2+}-free medium (Fig. 9*F*). The voltage responses to current steps still showed evidence for both inward and outward rectification, indicating the presence of TEA-insensitive conductances some of which may have been involved in repolarizing the cell membrane after the spontanteous action potentials and the plateau potentials in TEA plus Ca^{2+}-free medium.

Of ten type B cells tested with TEA followed by either low-Ca^{2+} Co^{2+} or Ca^{2+}-free Cd^{2+} medium, seven behaved as the example in Fig. 9. In the remaining three cells, however, the plateau potentials that developed in TEA were reduced in Ca^{2+}-free Cd^{2+} medium, as shown for one cell in Fig. 10. In this cell TEA again readily abolished the early fast AHP without affecting the slow AHP, and the spike developed a marked shoulder after a few minutes in 10 mM TEA (Fig. 10*A*, arrows). Instead of firing broad action potentials at a steady rate, however, the cell gradually depolarized and fired a series of broad action potentials at an increasing frequency, culminating in a single action potential with a plateau lasting over 1·5 s (Fig. 10*A*, arrowheads). With continued equilibration in 10 mM TEA, the number of spontaneous spikes with a long plateau potential increased, and those with only a shoulder decreased, until after 15 min in 10 mM TEA the cell regularly fired only single spikes with plateau potentials lasting 1·5–2 s (Fig. 10*B*). Subsequently, in Ca^{2+}-free Cd^{2+} medium containing 10 mM TEA these long plateau potentials were abolished and the cell again fired broad action potentials but now at a steady rate, with no tendency to increase in frequency as in TEA alone (Fig. 10*C*).

As shown in Fig. 10*E*, in 10 mM TEA this cell fired bursts of narrow action potentials superimposed on low-threshold, transient plateaux at a hyperpolarized membrane potential (Fig. 10*E*, arrows). These transient plateaux were not apparent before the cell was exposed to TEA (Fig. 10*D*) and were abolished in Ca^{2+}-free Cd^{2+} medium (Fig. 10*F*). The cell fired broad spikes in Ca^{2+}-free Cd^{2+} medium both at the resting membrane potential (Fig. 10*C*) as well as at a hyperpolarized potential (Fig. 10*F*), which were abolished in 0·5 μM TTX (not shown).

While the early fast AHP in type B cells was readily abolished in TEA (Figs 9 and 10), the late AHP was insensitive to TEA but was abolished in apamin (100 nM; Fig. 11, $n = 3$). Apamin did not affect the rate of repolarization of the action potential, nor the amplitude or duration of the fast AHP (Fig. 11*C*). The selective blockade of the slow AHP did not reveal any other membrane

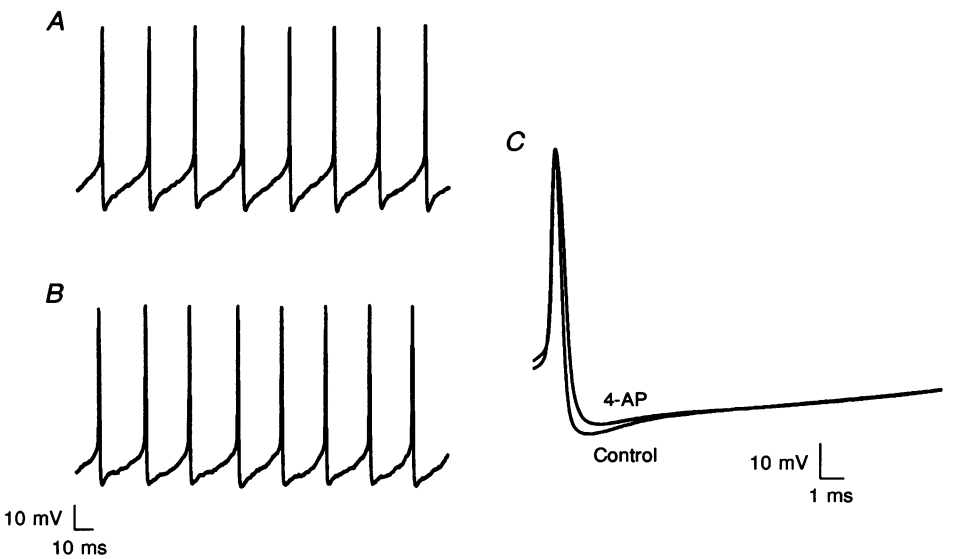

Figure 8. Effects of 4-AP on the tonic discharge and action potential shape of a type A cell
A, tonic discharge of the cell at its resting membrane potential of −51 mV in normal ACSF. *B*, tonic activity in 0·5 mM 4-AP. *C*, averaged spike shapes obtained during tonic activity in normal ACSF and in 4-AP superimposed.

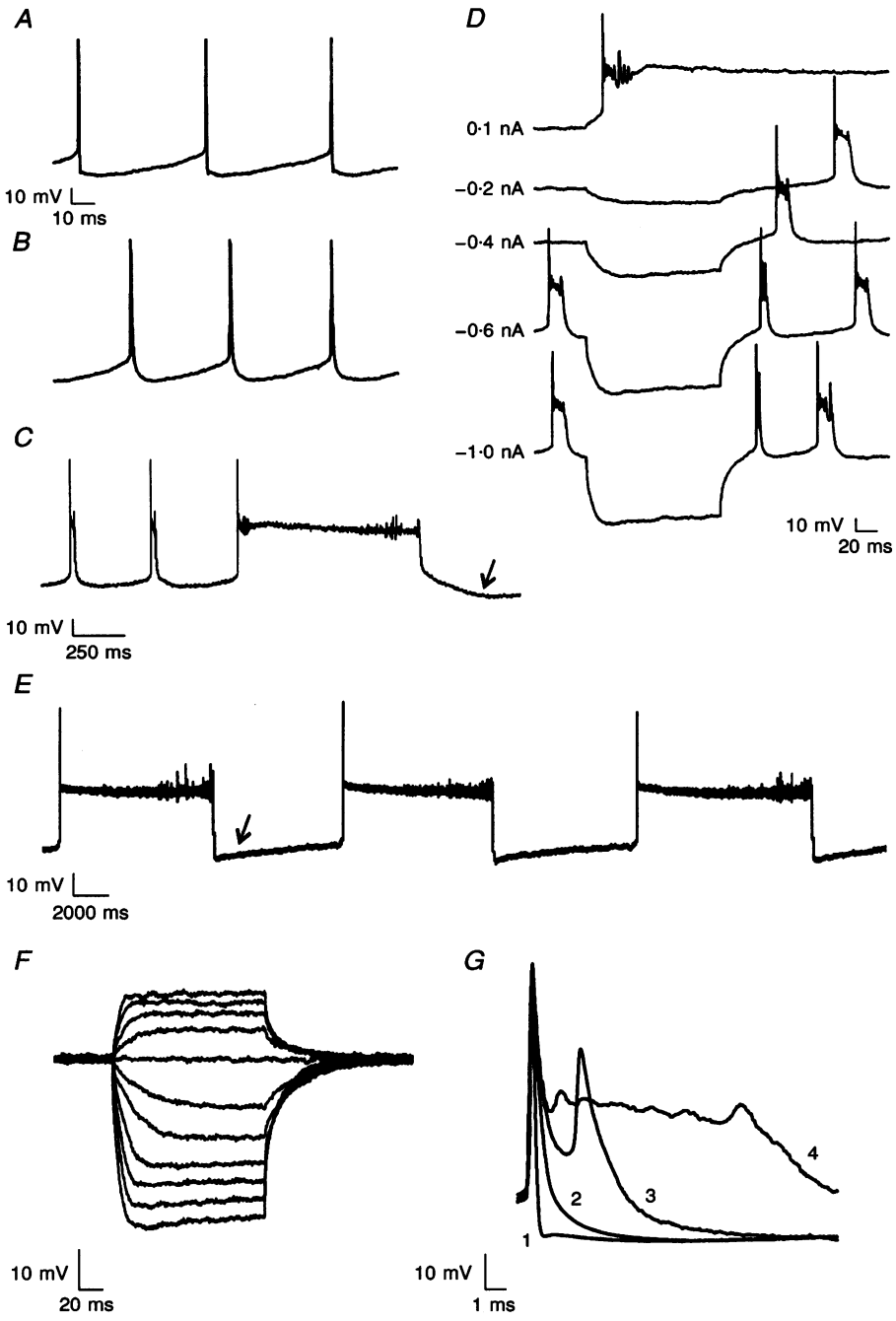

Figure 9. Effects of TEA and Ca^{2+}-free medium on action potential repolarization in a type B cell

A, resting discharge in normal ACSF; *B*, after 10 min in 5 mM TEA; and *C*, after 10 min in 10 mM TEA. In *C*, note broad spikes (first two) followed by a spike with a plateau that lasts 1·25 s. Arrow indicates deep AHP. *D*, responses to current pulses applied at a membrane potential of −65 mV after 8 min in 10 mM TEA. *E*, spontaneous action potentials in Ca^{2+}-free Cd^{2+} medium containing 10 mM TEA. Note plateaux lasting 7–9 s, and the ramp-like depolarization indicated by the arrow. *F*, responses of the same cell to current pulses in 0·5 μM TTX. *G*, spike shapes obtained during tonic activity in normal ACSF (trace 1), 5 mM TEA (trace 2), after 3 min in 10 mM TEA (trace 3) and after 15 min in 10 mM TEA (trace 4), superimposed. Traces 1 and 2 are averages of 38 and 52 spikes, respectively, while traces 3 and 4 are single spikes which were not averaged because successive spikes tended to vary somewhat in shape.

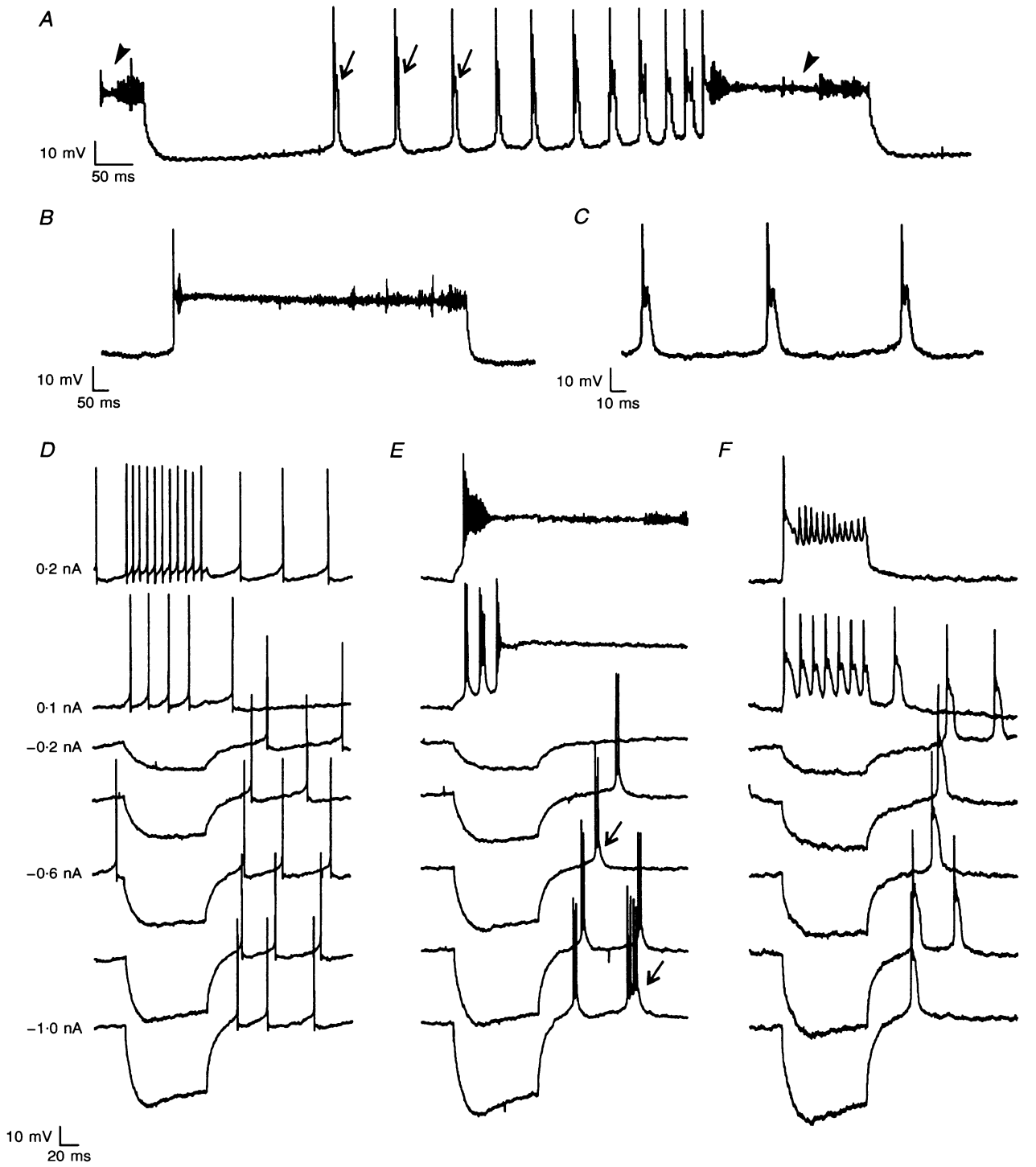

Figure 10. Effects of TEA and Ca^{2+}-free medium on action potential firing and repolarization in a different type B cell

A, spontaneous discharge at resting membrane potential (−55 mV) after 5 min in 10 mM TEA. Note broad spikes (arrows) firing at increasing frequency and culminating in a spike with a plateau lasting about 250 ms (arrowheads). *B*, typical spontaneous action potential after 12 min in 10 mM TEA. Note plateau lasting over 1 s. *C*, spontaneous action potentials after 25 min in Ca^{2+}-free Cd^{2+} medium containing 10 mM TEA. Note return to short plateaux with a smaller secondary spike. *D*, *E* and *F*, responses to current pulses in normal ACSF, 10 mM TEA and Ca^{2+}-free medium containing 10 mM TEA, respectively, at a membrane potential of −65 mV. Arrows in *E* indicate transient depolarizing plateaux with narrow spikes superimposed.

potential changes after the fast AHP. The regularity of the tonic discharge was lost after the blockade of the slow AHP in apamin (Fig. 11*B*), and the cells tended to fire irregular groups of closely spaced spikes. The slow AHP was also abolished in Ca^{2+}-free Cd^{2+} medium (Fig. 11*E*, $n = 4$; see also Figs 8 and 9). In contrast to the selective blockade of the slow AHP in apamin, however, in Ca^{2+}-free Cd^{2+} medium the fast AHP was also reduced by a small amount. While the selective blockade of the slow AHP by apamin caused irregular firing (Fig. 11*B*), the reduction of both fast and slow AHPs in Ca^{2+}-free Cd^{2+} medium resulted in burst-like behaviour in all four type B cells tested, with a series of closely spaced action potentials arising from a spontaneous depolarizing plateau (Fig. 11*D*).

4-AP (0·5 mM) caused a slowing in the rate of repolarization in type B cells, and abolished the fast AHP in a similar way to a low concentration (5 mM) of TEA (Fig. 12, $n = 3$). The slow AHP was potentiated in 4-AP, possibly due to its promotion of voltage-gated calcium influx (Rogawski & Barker, 1983). Unlike TEA, however, 4-AP did not have any further effects on the rate of repolarization and did not induce plateaux at higher concentrations. The regularity of the tonic discharge of the type B cells and the delay to the first action potential during a small depolarizing pulse from a hyperpolarized potential were again not changed in 0·5 mM 4-AP. When apamin and 4-AP were added together (Fig. 12*C* and *D*) both the fast and the slow AHPs were abolished but the cell still did not generate plateau potentials. Carbachol (50–100 μM) had no detectable effect on the rate of spike repolarization or the amplitude of the AHPs in four type B cells tested.

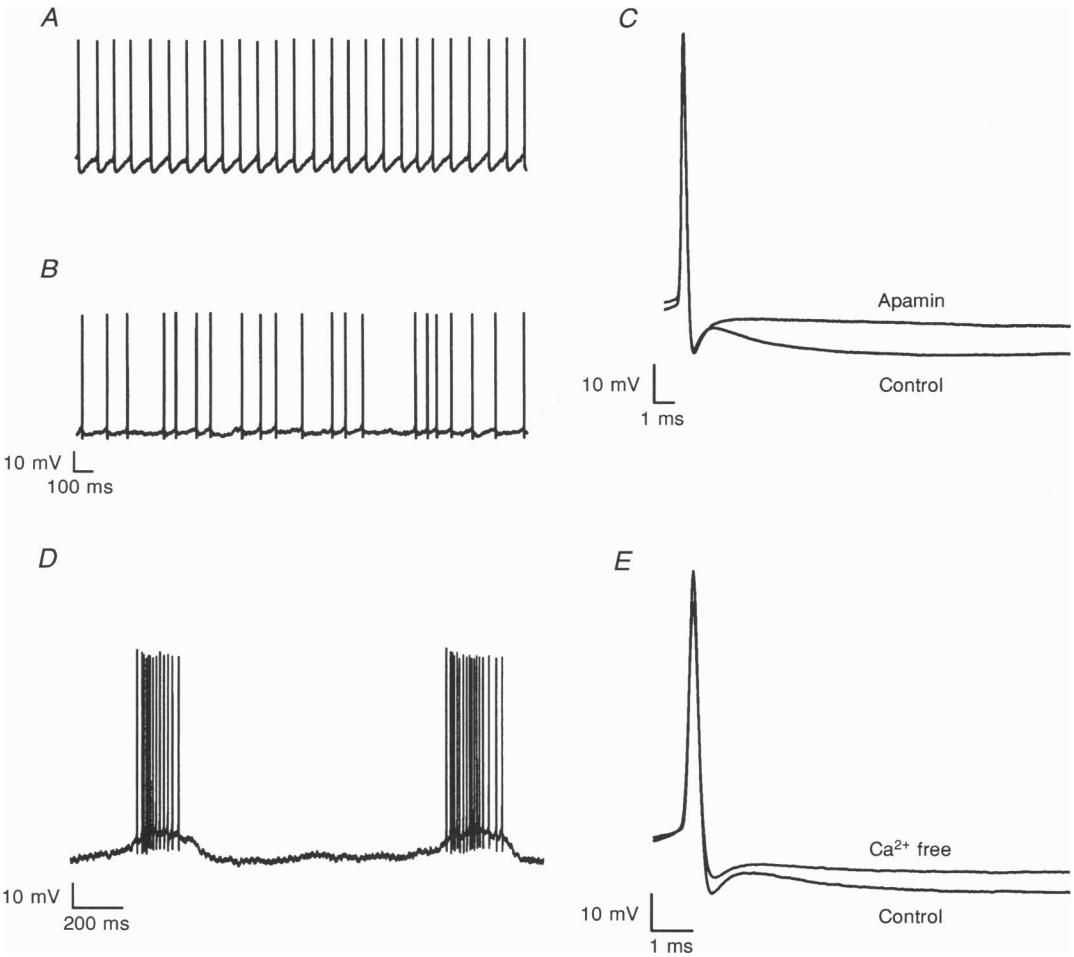

Figure 11. Effects of apamin (100 nM) on action potential firing and action potential shape of a type B MVN cell

A, control; *B*, irregular spiking after 7 min in apamin; and *C*, averaged spontaneous spikes in control and apamin medium superimposed. *D* and *E*, effects of Ca^{2+}-free medium on a second type B MVN cell. In *D*, the normal tonic discharge was replaced by burst-like firing after 25 min in Ca^{2+}-free medium. In *E*, averaged action potentials in control medium and in Ca^{2+}-free medium are superimposed. The cell was depolarized by current injection to elicit a steady discharge in Ca^{2+}-free medium, in order to obtain the spikes averaged in *E*.

DISCUSSION

Previous studies of the properties of rat and guinea-pig MVN neurones *in vitro* have suggested that while there were two major cell types in the nucleus distinguishable on the basis of their action potential shapes, a significant number of MVN cells had intermediate characteristics (Gallagher *et al.* 1985, 1992; Serafin *et al.* 1991*a*). A formal classification of MVN cells into three types (A, B and C) was proposed by Serafin *et al.* (1991*a*), in which types A and B corresponded to the two main types of action potential shape observed by Gallagher *et al.* (1985) and type C cells included those with intermediate properties. However, with the use of spike-shape averaging in the present study, all MVN cells were found to have either a single deep AHP characteristic of type A cells or a combination of a fast AHP followed by a delayed slow AHP characteristic of type B cells. The proportion identified as type A cells in the present study (40/123, 33%) is similar to that observed in the guinea-pig MVN by Serafin *et al.* (1991*a*), while the remaining cells (83/123, 67%) were identified as type B cells.

The relative prominence of the characteristic fast and slow AHPs in type B cells varied considerably between cells, and in many cases the two AHPs could only be clearly identified following the averaging of successive action potentials. The classification of action potential shape without spike-shape averaging was further complicated by the fact that the amplitude of the slow AHP in type B cells was dependent on the membrane potential (Fig. 3*B*), which tended to make it difficult to recognize in cells with high resting discharge rates. Thus, spike-shape averaging was effective in unambiguously classifying cells that initially appeared to have intermediate characteristics (type C cells), and it also proved useful in confirming the presence or absence of one or the other AHP in cells after selective ion-channel blockade. The present results show that MVN cells are essentially of two types, analogous with but not identical to the types A and B proposed by Serafin *et al.* (1991*a*), and demonstrate the necessity of spike-shape averaging in classifying them.

The two MVN cell subtypes identified on the basis of their averaged spike shapes also differed in the active membrane conductances involved in their tonic resting activity. The effects of TEA and Ca^{2+}-free medium on the rate of spike repolarization and the amplitude of the AHP in type A cells (Figs 5 and 6) indicate that a TEA-sensitive potassium conductance and a separate calcium-dependent outward conductance are involved. While TEA caused a uniform slowing of the rate of repolarization and an increase in spike width (Fig. 5), Ca^{2+}-free Cd^{2+} medium had only a small effect on the initial rate of repolarization but reduced the AHP amplitude markedly (Fig. 6). This suggests that the major part of action potential

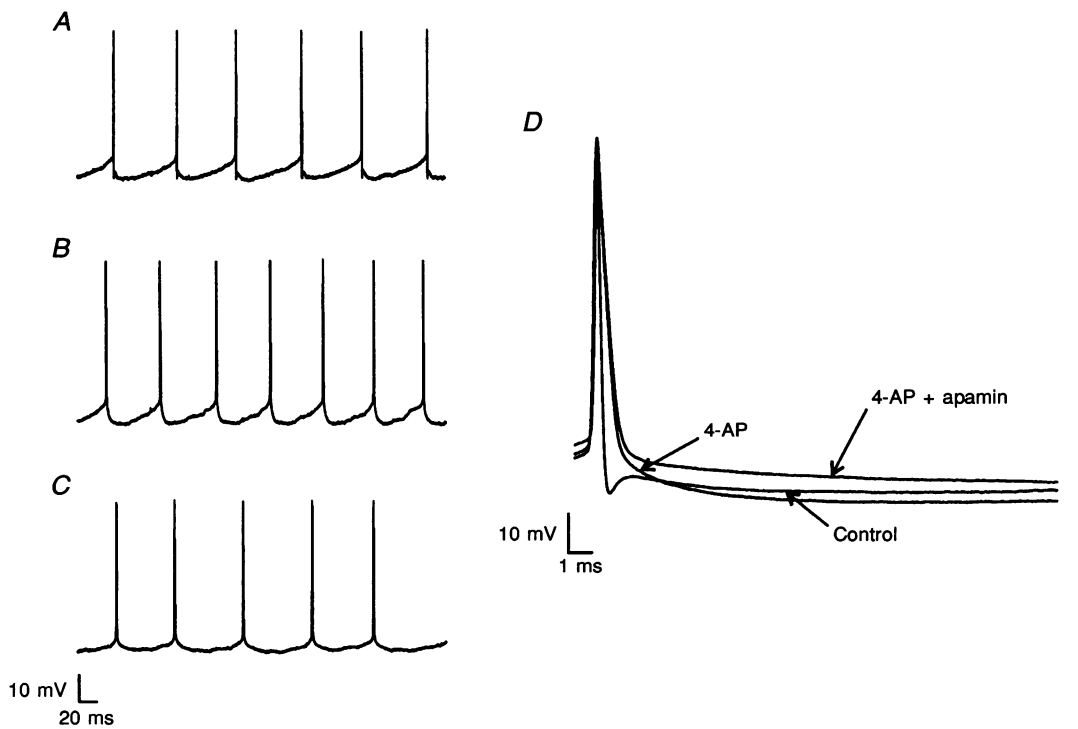

Figure 12. Effects of 4-AP and apamin on action potential firing and action potential shape of a type B MVN cell
A, control; *B*, after 12 min in 0·5 mM 4-AP; and *C*, after 10 min in 0·5 mM 4-AP and 100 nM apamin. *D*, averaged spikes in normal medium, 4-AP and 4-AP + apamin superimposed.

repolarization is mediated by a TEA-sensitive potassium conductance (presumably the voltage-gated I_K), while the deep AHP appears to involve, in addition, a calcium-dependent component, possibly the calcium-activated potassium conductance I_C.

While I_K and I_C are known to mediate spike repolarization in several neurone types (Llinás, 1988; Storm, 1990; Viana, Bayliss & Berger, 1993), in MVN type A cells the contribution of I_K to spike repolarization would appear to be much greater than that of I_C, at least at the level of the soma. Thus, the rate of repolarization in type A cells was uniform and did not show a Ca^{2+}-sensitive 'shoulder' observed in many cell types. The contribution of I_C to spike repolarization was also revealed only after I_K had been blocked by TEA, by the further uniform broadening of the spike in Ca^{2+}-free medium (Fig. 5). The small effect of apamin and the lack of effect of carbachol on the action potential shape in type A cells (Fig. 7) excludes the small-conductance (SK) type of calcium-activated potassium channels and the I_M subtype of potassium current from contributing significantly to spike repolarization in these cells (Phelan & Gallagher, 1992). The fact that 4-AP did slow the rate of repolarization and decreased the amplitude of the AHP by a small amount (Fig. 8) suggests that an A-like outwardly rectifying potassium current may play a part in spike repolarization in type A cells, although these effects may also be due to the weaker effects of 4-AP on other potassium conductances (for example see Galvan, Grafe & ten Bruggencate, 1982). Unlike type A cells in the guinea-pig MVN where such outward rectification was prominent in the response to depolarizing current pulses (Serafin *et al.* 1991*a*), none of the type A cells in this study showed a similar effect.

In type B cells, by contrast, the abolishment of the TEA-insensitive, delayed slow AHP in Ca^{2+}-free medium and its selective and complete blockade in apamin (Fig. 11) confirms that this is due to a calcium-activated potassium current involving calcium influx through the SK type calcium channels, similar to I_{AHP} described in bullfrog sympathetic ganglion cells (Pennefather, Lancaster, Adams & Nicoll, 1985) and in other cell types (Hille, 1991) and observed in guinea-pig type B MVN cells by de Waele, Serafin, Khateb, Yabe, Vidal & Muhlethaler (1993). The effects of membrane potential on this AHP (Fig. 3*B*) may be due to changes in calcium influx during action potentials rising from different levels of hyperpolarization. After the blockade of the delayed slow AHP the normal rhythmic discharge of type B cells was replaced by an irregular pattern of firing (Fig. 11), indicating that in the normal tonic activity of the cell the interspike hyperpolarization mediated by the calcium influx is an important factor in regulating the timing of successive spikes. In contrast, type A cells continued to fire regularly in Ca^{2+}-free medium, implying that the regularity in their tonic discharge may be less dependent on calcium-activated membrane conductances active near the resting membrane potential.

The fast AHP in type B cells was readily blocked by TEA, and after a few minutes in TEA these cells characteristically fired broad spontaneous action potentials with plateau potentials lasting up to 30 ms (Fig. 9). The effects of 4-AP, which were similar to a low concentration of TEA in blocking the fast AHP and slowing the rate of repolarization (Fig. 12). suggest that an A-type current may be involved in spike repolarization in type B cells, but this could also be due to a non-specific action of 4-AP on other potassium channels. Since the rate of spike repolarization in type B cells was not affected much in Ca^{2+}-free medium (Fig. 11) it would appear that, as in type A cells, the normal repolarization of the action potential in these cells is also largely due to a TEA-sensitive potassium current (presumably I_K). The fact that in the majority of type B cells the broad plateau potentials that developed after the blockade of I_K in TEA were not abolished in Ca^{2+}-free medium but instead became much longer in duration (Fig. 9), suggests that in the absence of I_K a slower, calcium-dependent process helps to terminate the plateaux during the steady firing of broad spikes. The development of the plateau potentials in TEA, and the steady ramp-like membrane depolarization immediately following the very long plateaux that developed in TEA plus Ca^{2+}-free medium, indicate that in type B cells there is a persistent inward conductance active near the resting membrane potential that constantly depolarizes them towards firing threshold. The interaction between this inward current and the remaining TEA-insensitive and calcium-independent outward currents tending to repolarize the cell may account for the partial repolarization of the action potential in Ca^{2+}-free medium plus TEA and the formation of the plateau potential (for discussion see Llinás & Sugimori, 1980; Stafstrom, Schwint, Chubb & Crill, 1985). Since the plateau potentials and the steady membrane depolarization were abolished in TTX (Fig. 9), the persistent inward current would appear to be a non-inactivating sodium conductance, similar to that observed in guinea-pig type B cells by Serafin *et al.* (1991*b*) and in other cell types (Llinás, 1988). Significantly, however, in about 30% of type B cells there would appear to be an additional low-threshold calcium conductance contributing to the membrane depolarization between successive spikes (Fig. 10). This conductance was not apparent in normal medium, but gave rise to transient plateau potentials and a slow membrane depolarization in TEA which were subsequently abolished in Ca^{2+}-free medium. These cells differed from the majority of type B cells in that the long plateau potentials that developed in TEA were reduced rather than potentiated in Ca^{2+}-free medium, and so were calcium rather than sodium dependent in a similar way to the after-depolarizing potentials seen in olivary nucleus cells (Llinás & Yarom,

1981). This subclass of type B cells remains to be characterized further.

While in type B cells the persistent membrane depolarizing conductances were large enough to give rise to plateau potentials when I_K was blocked in TEA, in type A cells the only indication of a similar mechanism was observed when these cells fired action potentials with short plateaux, sometimes with secondary spikes, in response to depolarizing pulses from a hyperpolarized membrane potential in TEA (Fig. 5). Since these short plateaux and the secondary spikes persisted in Ca^{2+}-free medium but were abolished in TTX, they also appear to be due to a non-inactivating sodium conductance. However, in type A cells this conductance is either not as large as in type B cells, or it is more effectively counteracted by TEA-insensitive outward currents than in type B cells, so that the long plateau potentials that occur in type B cells are not generated in type A cells. As a consequence, the pacemaker conductances that generate the tonic activity in the two types of MVN cell may rely on different mechanisms. In type B cells it seems reasonable to assume that the timing of successive spikes in the regular tonic discharge is regulated by interactions between the membrane depolarization caused by a persistent sodium conductance (with in 30% of cells an additional calcium conductance), and the hyperpolarization due to the calcium-activated potassium conductance I_{AHP} during the delayed slow AHP. By contrast in type A cells the depolarization of the membrane between action potentials may involve a persistent sodium current to a lesser extent, and be more dependent on the inactivation of potassium currents. While the present results suggest this fundamental difference between the two MVN cell types, further direct studies of these conductances under voltage clamp conditions are necessary.

REFERENCES

Blatz, A. L. & Magleby, K. L. (1986). Single apamin-blocked Ca^{2+}-activated K^+ channels of small conductance in cultured rat skeletal muscle. *Nature* **323**, 718–720.

Broussard, D. M. & Lisberger, S. G. (1992). Vestibular inputs to brain stem neurons that participate in motor learning in the primate vestibuloocular reflex. *Journal of Neurophysiology* **68**, 1906–1909.

Carpenter, R. H. S. (1988). *Movements of the Eyes*, 2nd edn. Pion, London.

de Waele, C., Serafin, M., Khateb, A., Yabe, T., Vidal, P. P. & Muhlethaler, M. (1993). Medial vestibular nucleus in the guinea-pig: apamin-induced rhythmic burst firing – an *in vitro* and *in vivo* study. *Experimental Brain Research* **95**, 213–222.

Dutia, M. B., Johnston, A. R. & McQueen, D. S. (1992). Tonic activity of rat medial vestibular nucleus neurones *in vitro* and its inhibition by GABA. *Experimental Brain Research* **88**, 466–472.

Gallagher, J. P., Lewis, M. R. & Shinnick-Gallagher, P. (1985). An electrophysiological investigation of the rat medial vestibular nucleus *in vitro*. In *Progress in Clinical and Biological Research*, vol. 176, ed. Correia, M. J. & Perachio, A. A., pp. 293–304. Alan R. Liss, New York.

Gallagher, J. P., Phelan, K. D. & Shinnick-Gallagher, P. (1992). Modulation of excitatory transmission at the rat medial vestibular nucleus synapse. *Annals of the New York Academy of Sciences* **656**, 630–644.

Galvan, M., Grafe, P. & ten Bruggencate, G. (1982). Convulsant actions of 4-amino-pyridine on the guinea-pig olfactory cortex slice. *Brain Research* **241**, 75–86.

Gustafsson, B., Galvan, M., Grafe, P. & Wigstrom, H. A. (1982). Transient outward current in mammalian central neurone blocked by 4-aminopyridine. *Nature* **299**, 252–254.

Halliwell, J. V. & Adams, P. R. (1982). Voltage-clamp analysis of muscarinic excitation in hippocampal neurons. *Brain Research* **250**, 71–92.

Hille, B. (1991). *Ionic Channels of Excitable Membranes*, 2nd edn. Sinauer, Sunderland, MA, USA.

Jahnsen, H. (1980). The action of 5-hydroxytryptamine on neural membranes and synaptic transmission in area CA1 of the hippocampus *in vitro*. *Brain Research* **197**, 83–94.

Johnston, A. R., Murnion, B., McQueen, D. S. & Dutia, M. B. (1993). Excitation and inhibition of rat medial vestibular nucleus neurones by 5-hydroxytryptamine. *Experimental Brain Research* **93**, 293–298.

Lisberger, S. G. & Pavelko, T. A. (1988). Brain stem neurons in modified pathways for motor learning in the primate vestibulo-ocular reflex. *Science* **242**, 771–773.

Llinás, R. (1988). The intrinsic electrophysiological properties of mammalian neurones: Insights into central nervous system function. *Science* **242**, 1654–1664.

Llinás, R. & Sugimori, M. (1980). Electrophysiological properties of *in vitro* Purkinje cell somata in mammalian cerebellar slices. *Journal of Physiology* **305**, 171–195.

Llinás, R. & Yarom, Y. (1981). Electrophysiology of mammalian inferior olivary neurones *in vitro*. Different types of voltage-dependent ionic conductances. *Journal of Physiology* **315**, 549–567.

Pennefather, P., Lancaster, B., Adams, P. R. & Nicoll, R. A. (1985). Two distinct calcium-dependent K currents in bullfrog sympathetic ganglion cells. *Proceeedings of the National Academy of Sciences of the USA* **82**, 3040–3044.

Phelan, K. D. & Gallagher, J. P. (1992). Direct muscarinic and nicotinic receptor-mediated excitation of rat medial vestibular nucleus neurons *in vitro*. *Synapse* **10**, 349–358.

Rogawski, M. A. & Barker, J. L . (1983). Effects of 4-amino-pyridine on calcium action potentials and calcium current under voltage clamp in spinal neurons. *Brain Research* **280**, 180–185.

Serafin, M., de Waele, C., Khateb, A., Vidal, P. P. & Muhlethaler, M. (1991*a*). Medial vestibular nucleus in the guinea-pig. I. Intrinsic membrane properties in brainstem slices. *Experimental Brain Research* **84**, 417–425.

Serafin, M., de Waele, C., Khateb, A., Vidal, P. P. & Muhlethaler, M. (1991*b*). Medial vestibular nucleus in the guinea-pig. II. Ionic basis of the intrinsic membrane properties in brainstem slices. *Experimental Brain Research* **84**, 426–433.

Smith, P. F. & Curthoys, I. S. (1989). Mechanisms of recovery following unilateral labyrinthectomy: A review. *Brain Research Reviews* **14**, 155–180.

SMITH, P. F., DARLINGTON, C. L. & HUBBARD, J. I. (1990). Evidence that NMDA receptors contribute to synaptic function in the guinea-pig medial vestibular nucleus. *Brain Research* **513**, 149–151.

STAFSTROM, C. E., SCHWINT, P. C., CHUBB, M. C. & CRILL, W. E. (1985). Properties of a persistent sodium conductance and calcium conductance of layer V neurons from cat sensorimotor cortex *in vitro*. *Journal of Neurophysiology* **53**, 153–170.

STORM, J. F. (1987). Action potential repolarization and a fast after-hyperpolarization in rat hippocampal pyramidal cells. *Journal of Physiology* **385**, 733–759.

STORM, J. F. (1990). Potassium currents in hippocampal pyramidal cells. In *Progress in Brain Research*, vol. 83, ed. STORM-MATHISEN, J., ZIMMER, J. & OTTERSEN, O. P., pp. 161–187. Elsevier, Amsterdam.

VIANA, F., BAYLISS, D. A. & BERGER, A. J. (1993). Calcium conductances and their role in the firing behaviour of neonatal rat hypoglossal motoneurons. *Journal of Neurophysiology* **69**, 2132–2149.

WILSON, V. J. & MELVIL-JONES, G. (1979). *Mammalian Vestibular Physiology*. Plenum Press, New York.

Acknowledgements

This work was supported by project grant no. 018707/1.5 from the Wellcome Trust.

Received 20 December 1993; accepted 7 April 1994.